Magazine of Civil Engineering. 2020. 97(5). Article No. 9708

Magazine of Civil Engineering

ISSN 2071-0305

journal homepage: http://engstroy.spbstu.ru/

DOI: 10.18720/MCE.97.8

Behavior of CFRP strengthened columns damaged by thermal shock

R. Al-Rousan*

Jordan University of Science and Technology, Irbid, Jordan

** E–mail: rzalrousan@just.edu.jo*

Keywords: reinforced concrete, thermal shock, structural strength, axial strength, fiber reinforced polymer, nonlinear, finite element analysis

Abstract. In the last two decades, using of Carbon Fiber Reinforced Polymers (CFRP) in strengthening of deficient reinforced concrete structural elements has been increased due to their ease of installation, low invasiveness, high corrosion resistance, and high strength to weight ratio. Strengthening damage structures is a relatively new technique. This paper presents a nonlinear finite element analysis (NLFEA) results of reinforced concrete columns confined externally with carbon fiber reinforced polymers (CFRP) subjected to thermal shock impact. After reasonable validation of NLFEA with the experimental test results of companion columns, NLFEA was expanded to provide a parametric study of eighteen columns that correlates the ultimate axial stress of CFRP-confined RC columns to number of CFRP layers and damaged thermal shock. Thermal shock has a significant impact on the behavior of CFRP-confined circular RC columns. The increase in ductility is directly related to a decrease of compressive strength due to thermal shock. Also, the confinement effectiveness in terms of ultimate load was decreased with the increase in concrete compressive strength (un-damaged). The influence of the number of CFRP layers on the ductility, energy absorption, and ultimate load improvement percentage is significant. There will be no further significant increase in the ductility and ultimate load of the column after a certain volumetric ratio, while significant increase in its stiffness continues to occur.

1. Introduction

It is inevitable to strengthen and/or retrofit concrete structural elements in order to prevent their potential vulnerability. One common procedure is confining such elements with CFRP wraps, which completely limit the lateral expansion of concrete and delay concrete cover peeling and longitudinal bars buckling. The general influence is clearly an increase in the peak loads of the specimens. Most studies in this area have been focused on column behavior under concentric and eccentric loads [1, 2]. It is necessary to strengthen the deteriorated and damaged reinforced concrete columns due to the overloads from earthquake and environmental conditions. Steel plate jackets and reinforced concrete jackets have been widely used to strengthen the RC columns. However, they have several problems because of their material characteristics, longer construction period due to curing requirement and the enlargement of column size. To solve the above problems, CFRP composites have been used for confinement of concrete since the early 1980's. External confining of concrete with CFRP composites is an efficient repair technique to enhance their strength and ductility due to the extreme high strength to weight ratio, the ease and speed of installation and application, and good corrosion behavior. Issa and Tobaa studied the strength and ductility enhancement in high-strength confined concrete columns. They concluded that the increase in the effective lateral pressure and post-peak ductility of the transverse steel decreases the slope of the descending branch of the stress-strain curve of the confined concrete [3].

Elevated temperatures cause severe damage for reinforced concrete (RC) structures, such as RC beams. RC beams have been reported to loss strength and stiffness with relatively large permanent deformations because of exposure to high temperatures [4]. These harmful effects could be attributed to the deterioration of mechanical characteristics of concrete and steel rebars and the redistribution of stresses within the beam due to the elevated temperatures [4, 5]. Currently, the most commonly used technique to repair the heat-damaged RC beams is using carbon fiber reinforced polymer (CFRP) composites. These sheets are advanced materials that can be easily applied on the structures and characterized by outstanding mechanical and corrosion resistance characteristics. Various studies were performed to investigate the flexural behavior

Al-Rousan, R. Behavior of CFRP strengthened columns damaged by thermal shock. Magazine of Civil Engineering. 2020. 97(5). Article No. 9708. DOI: 10.18720/MCE.97.8

of RC beams wrapped with CFRP. The results showed that externally bonded carbon FRP (CFRP) sheets and laminates has the ability to enhance the flexural behavior of the beams and recover, to certain limit, the flexural strength of heat-damaged beams. Strengthening level or recovery depends on several factors such as fire resistance [6], elevated temperature [7, 8], fiber type [9−12], analysis analysis type [13−17], energy integrity resistance [18], anchored system [20], heating condition [21, 22], degree of beam's damage and geometry and type of fiber sheet [23], and safety factors for CFRP strengthening of bridges [24].

Reinforcing concrete structures are often subjected to cycles of heating–cooling such as in chimneys, concrete foundations for launching rockets carrying spaceships, concrete near to furnace, clinker silos and nuclear power plants, or those subjected to fire then extinguished using water. Temperature cycles are critical to the stability of concrete structures and require considerations upon design [25, 26]. As well stipulated, the mechanical properties of concrete are preserved for exposure temperatures below 300°C, yet are decreased considerably as temperature exceeds 500 °C. Additional damage results from rabid cooling such as in the case of distinguishing of fire with cool water due to creation of temperature gradient between concrete core and its surface. This results in tensile stresses on the concrete surface that are high enough to crack concrete and this considered as another source of damage results from incompatible expansion and contraction of aggregate and surrounding cement paste. The magnitude of damage is influenced by many factors such as the size of concrete members, the type of cement and aggregate, the concrete moisture content and the predominant environmental factors, Those are represented in heating exposure time and rate, type of cooling, and maximum temperature attained [27]. Different types of materials and techniques were used in strengthening and retrofitting of existing concrete structures such as steel plates bolting, reinforced concrete jackets, pre-stressed external tendons, and most recently FRP composite which has been used on a large scale in different countries. FRP composites have many advantages over conventional methods represented in ease of application, high strength-to-weight ratio, excellent mechanical strength, and good resistance to corrosion, especially that most structures are damaged due to dynamic loads, corrosion of steel, and freeze-thaw cycles [28, 29].

Many reinforced concrete bridges are deteriorating due to problems related to environment and increase in load of trucks. In the last twenty years, considerable attention has been focused on the use of CFRP for structural rehabilitation and strengthening. Therefore, essential issues to produce effective, economical, and successful CFRP strengthening were needed. Also, the impact of CFRP external strengthening on the behavior of deficient reinforced concrete columns damaged by thermal shock must receive miniature consideration. The scientific problem considered in the study is indeed one of the problems in the modern theory of deficient reinforced concrete columns. A lack of literature regarding behavior of deficient columns damaged by thermal shock necessitated conducting the present investigation. In this study, experimental and NLFEA program were carried out to find the improvements in the strength and ductility behavior of reinforced concrete (RC) columns confined externally with CFRP composites. The main parameters studied were number of CFRP layers (Volumetric ratio) and thermal shock impact.

2. Methods

ANSYS V16 software is an effective numerical method and important tool in the analysis of complex structures. The main benefits that NLFEA include: 1) substantial savings in the cost, time, and effort compared with the fabrication and experimental testing of structure elements; 2) allows to change any parameter of interest to evaluate its influence on the structure, such as the concrete compressive strength; 3) allows to see the stress, strain, and displacement values at any location and at any load level. Eighteen full-scale models strengthened using CFRP are developed to carry out different investigated parameters.

2.1. Experimental work review

The validation process of the finite element model is based on the experimental work performed by Issa et al. [30]. CFRP-confined circular RC columns of 750 mm in length and 150 mm in diameter were fabricated and tested to failure. All columns were longitudinally reinforced with 4#3 steel bars (ρ = 1.56 %) and laterally reinforced with spiral steel reinforcement, 4.75 mm in diameter, spaced at 75 mm center to center along the entire height of the columns. The spacing of the spirals of 75 mm on center was based on the volumetric spiral reinforcement ratio. The ends of the columns were strengthened with additional two layers of CFRP-sheets for a distance of 125 mm from each end to prevent premature failure at the ends due to stress concentration. The reinforcement details, cross section, and the CFRP confinement configurations of the un-damaged columns are shown in Fig. 1. The CFRP-strengthened columns included columns strengthened with 1 (CS1-UD), 2 (CS2-UD), 3 (CS3-UD), 4 (CS4-UD), and 5 (CS5-UD) layers of CFRP in the transverse direction (Fig. 1). The 28-day cylindrical concrete compressive strength is 55 MPa. The yield stress of the longitudinal and spiral steel reinforcements was 410 MPa. The carbon fiber used was unidirectional in the form of tow sheet, manufactured in wide strips with a tensile strength of 3800 MPa and an elastic modulus of 230 GPa. The specimens were tested in the vertical position under axial compression loading in a special fabricated rigid steel frame. The test setup was designed to simulate pinned-pinned conditions (spherical shape) at both

ends of the columns. The specimens were centered and aligned with the help of lead shims that were laid between the column end and the steel plates to take up possible discrepancies and to ensure an even load distribution.

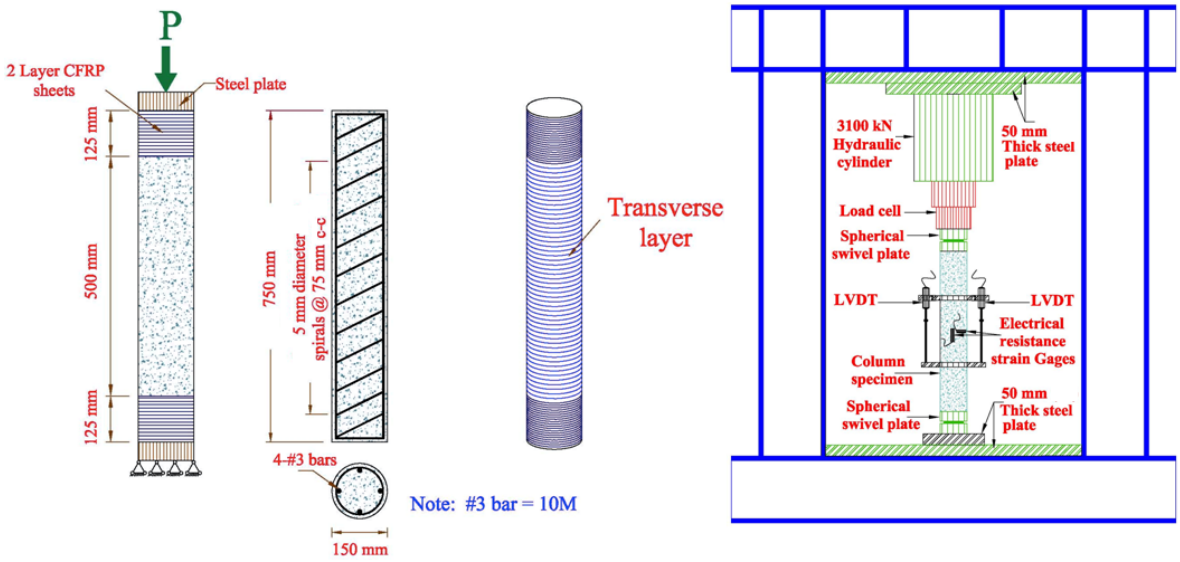

Figure 1. Setup and reinforcement details of the Columns [30].

2.2. Description of non-linear finite element analysis (NLFEA)

Concrete is non-homogenous and brittle material and has different behavior in tension and compression. SOLID 65 element is capable to predict the nonlinear behavior of concrete materials by using a smeared crack approach by ultimate uniaxial tensile and compressive strengths. The average compressive strength of the cylinders before and after being damaged by thermal shock were 55 and 10 MPa, respectively, and the average splitting tensile strength of the cylinders before and after being damaged by thermal shock were 2.9 and 0.7 MPa, respectively [31]. Poisson's ratio of 0.2 and shear transfer coefficient (β_t) of 0.2 for β_t was used in this study. Fig. 2(a) shows the stress-strain relationship for unconfined concrete which describes the post-peak stress-strain behavior.

LINK180 element was used to model the steel reinforcement. The 3-D spar element is a uniaxial tension-compression element with three degrees of freedom at each node with translations in the nodal x, y, and z directions. The element is also capable of plastic deformation. The steel in simulated models was assumed to be an elastic-perfectly plastic material and the same in compression and tension. Poisson's ratio of 0.3 and the yield stress of undamaged and damaged columns were 410 MPa and 0.78 f_y [32], respectively, as well as the elastic modulus were 200 GPa and 0.6 E_s [32], respectively, were used for the steel reinforcement. Fig. 2 (b) shows the idealized stress-strain relationship. The steel plates were assumed to be linear elastic materials with a Poisson ratio and elastic modulus of 0.3 and 200 GPa, respectively. The CFRP sheet is assumed to be an orthotropic material 0.17 mm thick, tensile strength of 3800 MPa, elastic modulus of 230 GPa, and ultimate tensile strain of 0.0169 as shown in Fig. 2 (c).

The contact area between the concrete and CFRP composite was modeled by a CONTA174 element. In this study, the bond stress-slip model between CFRP plates and damaged concrete by thermal shock proposed by Haddad and Al-Rousan [33] was used as shown in Fig. 3. Full column was simulated to study the behavior of the control reinforced concrete column. By taking advantage of symmetry of the column and loadings, a quarter of the full column was used in the analysis with proper boundary conditions, which reduced the computing time and computer disk space requirements. To simulate the pinned-pinned condition at both ends, one end was modeled as pin support, while only translation in the loading direction and rotation were allowed at the other end (point of load application). A convergence study was carried out to determine the appropriate mesh density. Perfect bonding was assumed between the composite column elements. Fig. 4 shows a typical finite element meshing of all columns. The total load applied was divided into a series of load increments or load steps. Newton-Raphson equilibrium iterations provide convergence at the end of each load increment within tolerance limits equal to 0.001 with load increment of 0.35 kN.

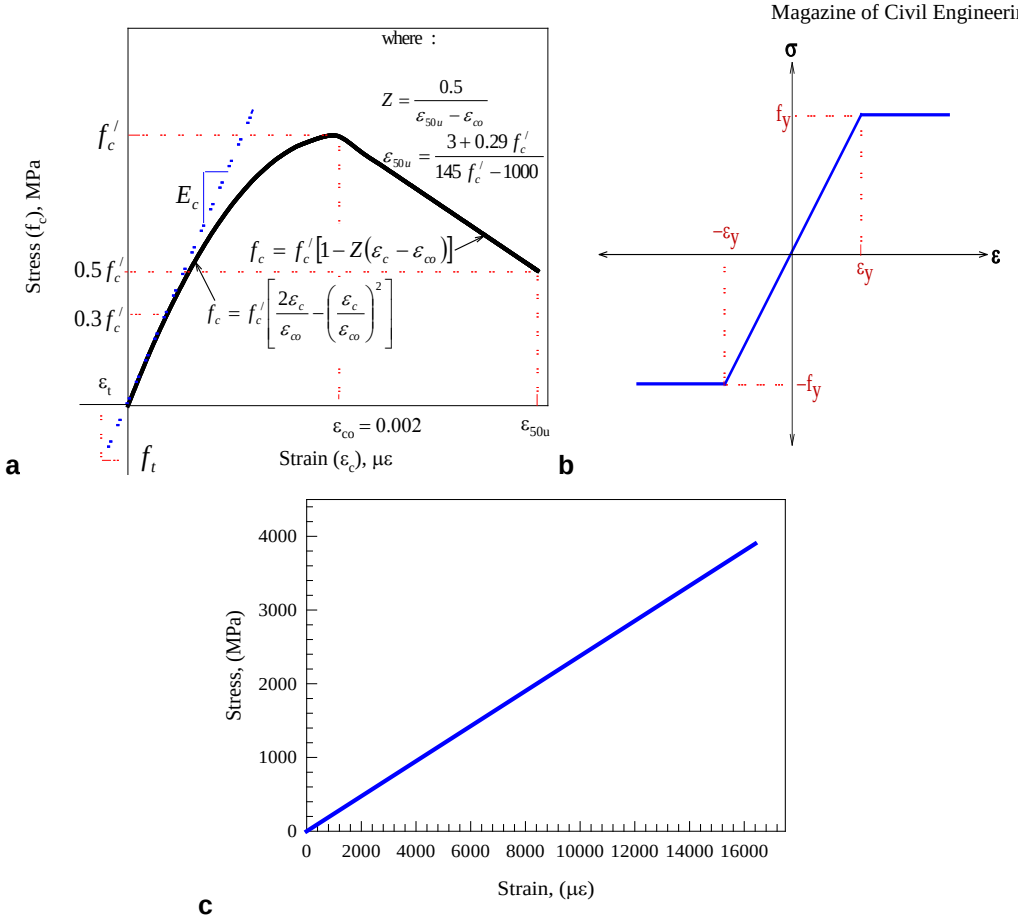

Figure 2. Stress-strain curves for: (a) unconfined concrete [30], (b) steel reinforcement [32], and CFRP composite.

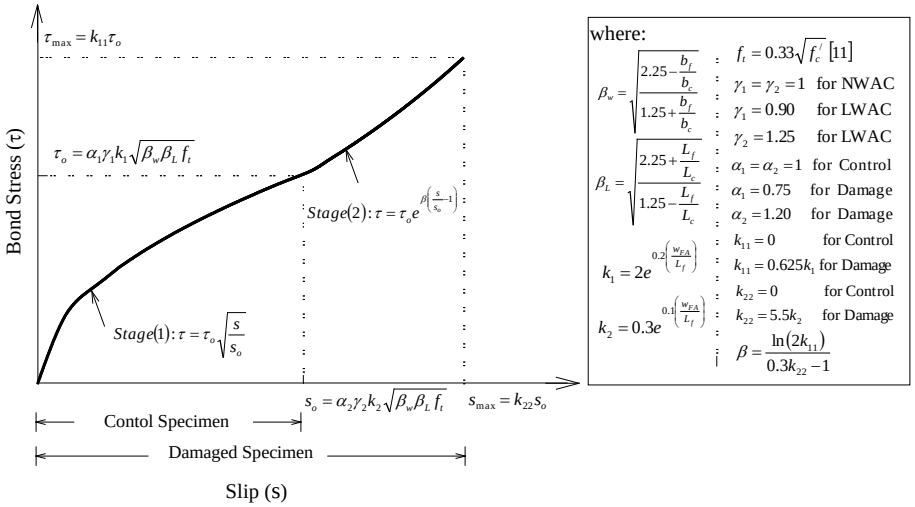

Figure 3. CFRP to concrete bond slip model [33].

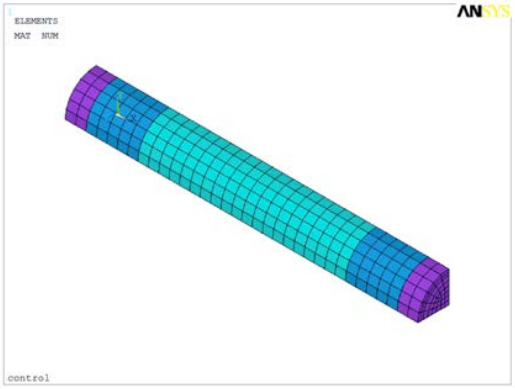

Figure 4. Typical finite element meshing of the Column.

2.3. Investigated Parameters

Table 1 shows configuration of different strengthening techniques, where unlike one un-damaged control column (CC-UD) and one control damaged column (CC-D), and the other sixteen columns were strengthened in shear using CFRP sheets as follows: CS1-UD and CS1-D (undamaged and damaged, respectively) were strengthened with one layer of CFRP (750 mm wide×0.17 mm thick). CS2-UD and CS2-D (undamaged and damaged, respectively) were strengthened with two layer of CFRP (750 mm wide×0.34 mm thick). CS3-UD and CS3-D (undamaged and damaged, respectively) were strengthened with three layer of CFRP (750 mm wide×0.51 mm thick). CS4-UD and CS4-D (undamaged and damaged, respectively) were strengthened with four layer of CFRP (750 mm wide×0.68 mm thick). CS5-UD and CS5-D (undamaged and damaged, respectively) were strengthened with five layer of CFRP (750 mm wide×0.85 mm thick). CS6-UD and CS6-D (undamaged and damaged, respectively) were strengthened with six layer of CFRP (750 mm wide×1.02 mm thick). CS7-UD and CS7-D (undamaged and damaged, respectively) were strengthened with seven layer of CFRP (750 mm wide×1.19 mm thick). Finally, CS8-UD and CS8-D (undamaged and damaged, respectively) were strengthened with eight layer of CFRP (750 mm wide×1.36 mm thick). A full description of the finite element modeling groups is shown in Table 1.

Table 1. NLFEA results of confined columns with CFRP composites.

Group Number	Number of CFRP layers	Volumetric ratio	Column number	Un-damaged/ Damaged	CFRP strengthening configuration	Ultimate load, kN
1	0	0	CC-UD	Un-damaged	Control column without strengthening	1161
	1	0.00433	CS1-UD		Column strengthened with one layer of CFRP	1628
	2	0.00867	CS2-UD		Column strengthened with two layer of CFRP	2077
	3	0.01300	CS3-UD		Column strengthened with three layer of CFRP	2420
	4	0.01733	CS4-UD		Column strengthened with four layer of CFRP	2700
	5	0.02167	CS5-UD		Column strengthened with five layer of CFRP	2891
	6	0.02600	CS6-UD		Column strengthened with six layer of CFRP	3060
	7	0.03033	CS7-UD		Column strengthened with seven layer of CFRP	3211
	8	0.03467	CS8-UD		Column strengthened with eight layer of CFRP	3336
2	0	0	CC-D	Damaged	Control column without strengthening	422
	1	0.00433	CS1-D		Column strengthened with one layer of CFRP	711
	2	0.00867	CS2-D		Column strengthened with two layer of CFRP	946
	3	0.01300	CS3-D		Column strengthened with three layer of CFRP	1116
	4	0.01733	CS4-D		Column strengthened with four layer of CFRP	1248
	5	0.02167	CS5-D		Column strengthened with five layer of CFRP	1331
	6	0.02600	CS6-D		Column strengthened with six layer of CFRP	1393
	7	0.03033	CS7-D		Column strengthened with seven layer of CFRP	1435
	8	0.03467	CS8-D		Column strengthened with eight layer of CFRP	1461

Note: C: Column, UD: un-damaged, D: Damaged

2.4. Validation Process

The experimental work included the fabrication of fifty-five circular reinforced concrete columns confined externally with various number and configurations of CFRP sheets. The columns were instrumented and tested to failure under pure axial loading. In addition, NLFEA was used to model the structural behavior of these columns. Fig. 5 shows the axial loads versus axial displacement behaviors for the simulated and tested columns. The axial load displacement curves shown in Fig. 5 (a), reveals that there is a significant increase in the ultimate axial load as well as in the ultimate axial displacement when confining the circular columns with CFRP sheets. Fig. 5 (a) also shows that the increase in the ultimate loads and displacements is directly related to an increase in the number of CFRP sheet layers. Also, Fig. 5 (b) shows the axial load versus axial and circumferential strains for the simulated columns.

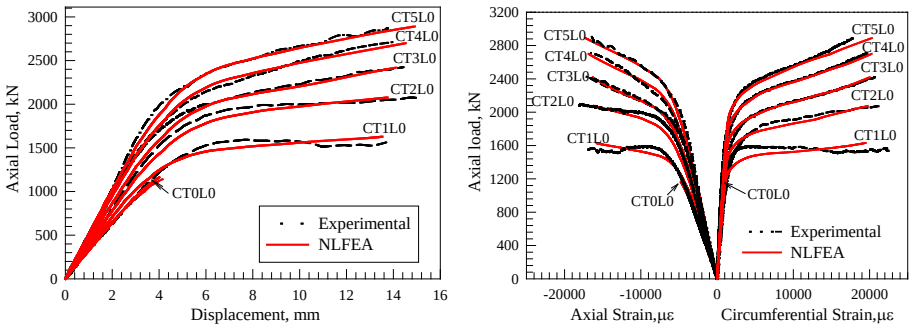

(a) **(b)**

Figure 5. Axial load vs. (a) axial displacement and (b) circumferential strain curves.

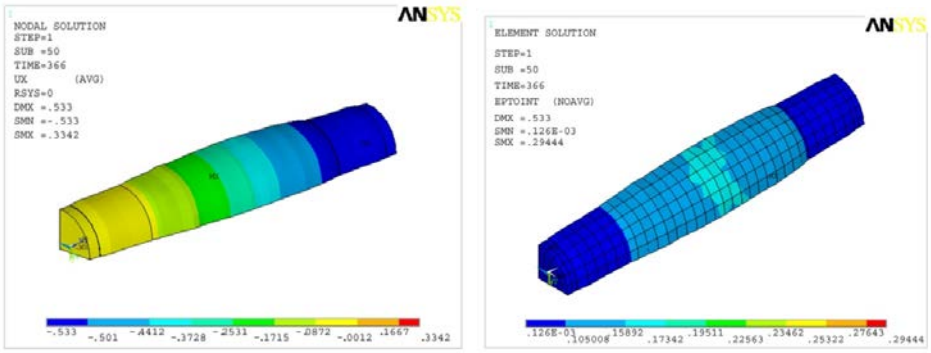

(a) **(b)**

Figure 6. Typical NLFEA contours for (a) control column and (b) column confined with 1 layer of CFRP composites.

The axial load axial strain behavior followed a similar trend as the axial load axial displacement for each specimen. At failure, the circumferential strain readings of the confined columns were greater than 0.017 mm/mm, which is the maximum strain capacity of the carbon fiber. The circumferential strain results coincide with the observed failure mode of the confined columns, the failures did not occur before fracturing of the CFRP sheets. This shows that the effectiveness of the CFRP confinement was good. As a result, there is good agreement between the NLFEA and the experimental test results. The general behaviors of the simulated columns show good agreement with observations and data from the experimental full-scale column tests with an average percentage of less than 5 %. Fig. 6 shows a typical NLFEA deformed shape and circumferential strain contours for column confined with 1 layer of CFRP composites. It was suggested to use NLFEA for further research on numerical tests and parametric analysis to provide theoretical understanding for establishing the stress strain curve model.

3. Results and Discussion

3.1. Failure Mode

The typical failure of the NLFEA specimens was initiated by fracture of the CFRP sheets at or near the center of the specimen (Fig. 6). The failure at the extreme edges was not of consequence as the ends were strengthened at these locations. When the load approached the ultimate load, circumferential fracture of the carbon fiber sheets was occurred that leads to a sudden release of energy. The specimen experienced a significant loss in resistance as the CFRP sheets began to fail followed by the fracturing of lateral reinforcement

and buckling of the longitudinal reinforcement. Similarly, failure of the control columns occurred due to the fracturing of the lateral reinforcement followed by buckling of the longitudinal reinforcement.

3.2. Loading behavior stages

The loading behavior of the specimens wrapped with CFRP can be divided into three stages. The first stage A is from zero applied load to 0.65 N_p (N_p is the peak load of each wrapped column) as shown in Fig. 7. In this stage, all curves are almost the same. Lateral expansions were very small and the fiber stresses were low (10 % of their ultimate strength). The second Stage B is from 0.65 N_p to 0.8 N_p. At this stage, the steel bars and spirals have yielded. The spirals reached their ultimate strain, the concrete started to have a large expansion, and the fiber begins to be stressed and crushing of the concrete at the end of this stage. After 0.8 N_p, the third Stage C started with large deformation in the axial and lateral directions and a slow rise in load. The load was carried by the CFRP composite after crushing of the concrete until the fiber fractured.

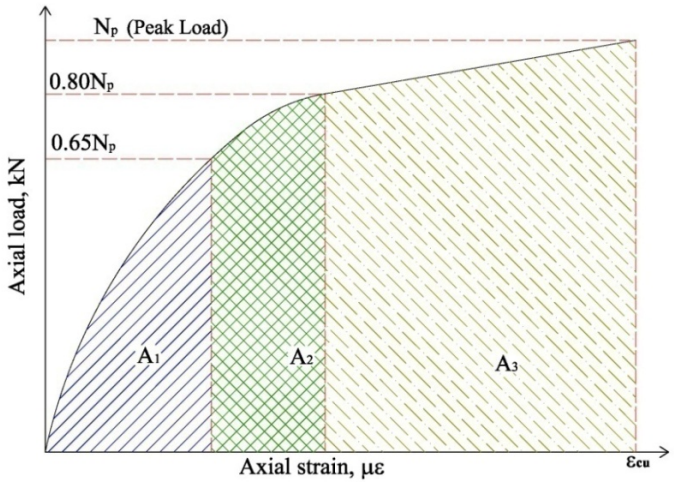

Figure 7. Typical loading behavior stages of the NLFEA columns.

To understand the contribution of each stage, energy absorption (EA) was calculated as the area under the load-displacement curve up to ultimate capacity. The area under the axial load-axial displacement curve was divided into three parts to measure the energy absorption during each stage as shown in Fig. 7. A_1, which represent the area from zero applied load to 0.65 N_p (Stage A), A_2 is the area from 0.65N_p applied load to 0.80 N_p (Stage B), and A_3 is the area from 0.80 N_p applied load to N_p (Stage C). Fig. 8 shows the normalized energy absorption for all stages with respect to the total energy for damaged and un-damaged columns. Inspection of Fig. 8 reveals that the energy absorption by CFRP composite after crushing of the concrete until the fiber fractures during stage C is about 65−70 % of total energy. Also, the EA only begins decreasing with the number of CFRP layers after seven layers. Until that point, EA increases with increasing number of layers. Stages A and B, which almost have equal absorption energy is about 30−35 % of total energy and increases with an increase in number of layers. Also, the total absorption energy of the composite system has the same trend as Stage C, which reflects the essential occupation of CFRP composite on the behavior of the wrapped column. Inspection of Fig. 8 reveals that the average EA reduction percentage due to thermal shock is 45 %.

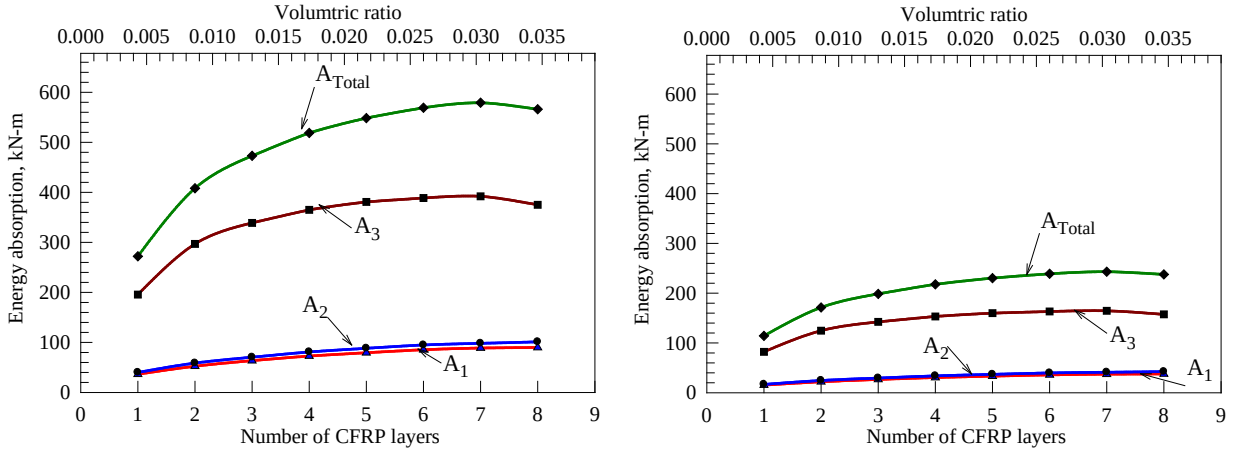

Figure 8. Energy absorption versus number of CFRP layers for (a) Un-damaged and (b) Damaged confined columns.

3.3. Effect of the number of transverse CFRP layers

To determine an enhancement in ductility between the control and CFRP confined columns, the areas under the axial load-axial displacement curves shown in Fig. 5(a) were computed. The energy absorption (EA) is plotted versus CFRP volumetric ratio as shown in Fig. 9. A polynomial relationship was observed with high correlation coefficient of 0.996 and is presented in Fig. 9. Depending on the CFRP volumetric ratio of the circular column and compressive strength of concrete, this relationship can be utilized to calculate the required energy absorption. In addition, the ductility of the RC columns can be calculated as the normalized energy absorption with respect to the energy absorption of control RC column. From this relationship, the energy absorption increases with increasing number of CFRP layers. The percentage of increase in ultimate load (Table 1) with respect to the control column was calculated as shown in Fig. 10. Inspection of Fig. 10 reveals that the rate of strength gain is reduced with increase in CFRP layers. This mean, after a certain volumetric ratio, there would be no further significant increase in the ductility behavior (Fig. 9) and ultimate load (Fig. 10) of the column, while significant increasing in its stiffness continues to occur (Fig. 5(a)). In addition, the increase in stiffness has led to decrease in lateral expansions of fiber stresses (Fig. 5(b)), delays in the spiral and steel yielding, and increases in concrete crushing load.

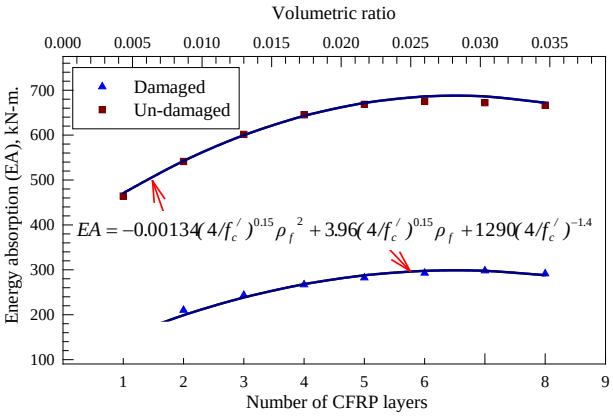

Figure 9. Energy absorption (EA) versus number of CFRP layers.

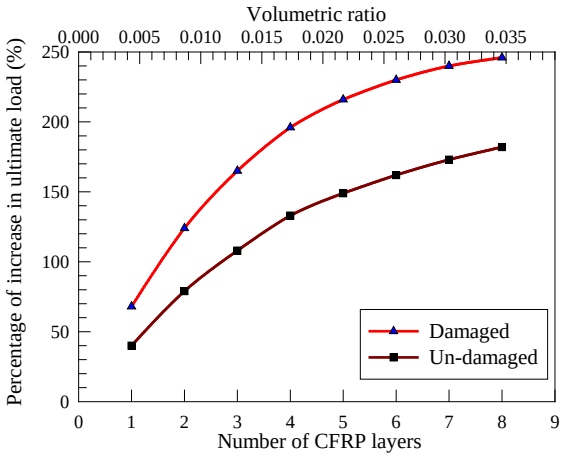

Figure 10. Ultimate load improvement percentages versus number of CFRP layers of confined columns.

3.4. Dilation properties

Fig. 11 shows the average volumetric curves versus the axial stress for NLFEA confined columns with CFRP composites. Inspection of Fig. 11(a) reveals that for un-damaged columns, one to six CFRP layers do not provide adequate confinement pressure to resist the dilation tendency of concrete. Alternatively, for the same column, seven to eight reverse the dilation trend of concrete (Compaction). While, one to three CFRP layers for damaged columns do not provide adequate confinement pressure to resist the dilation tendency of concrete. On the other hand, for the same column strength, four to eight reverse the dilation trend of concrete (Compaction). Therefore, the minimum amount of CFRP for sufficient confinement was four and seven layers of CFRP for damaged and un-damaged columns, respectively. It can be concluded that the number of CFRP layers that provide sufficient confinement to resist the dilation of concrete increased with the decrease of concrete compressive strength due to thermal shock.

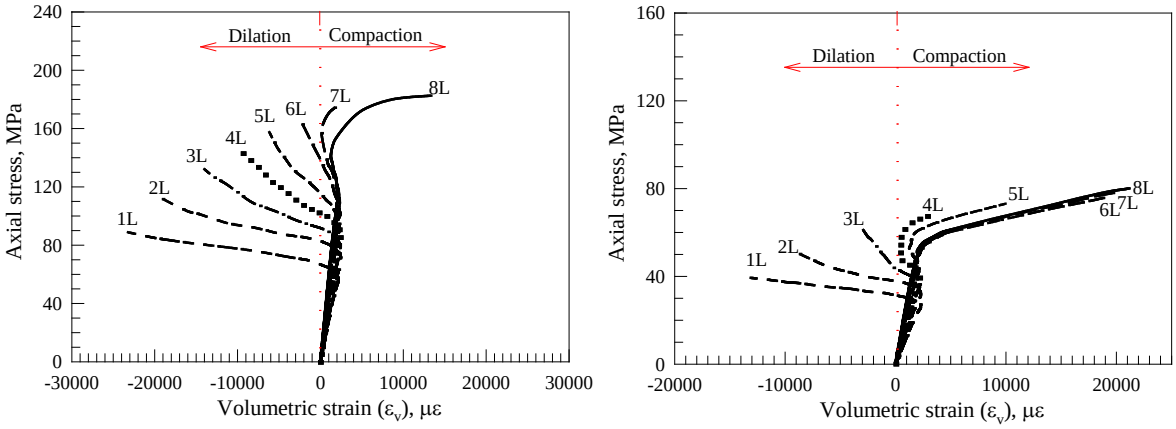

Figure 11. Volumetric strains for (a) Un-damaged and (b) Damaged confined columns.

3.5. Column ductility

The concept of ductility is related to the ability of a structural member to sustain inelastic deformation without substantial decrease in the load carrying capacity. Particularly, when it comes to reinforced concrete columns, ductility is an important issue due to their brittle failure mode. The ductility and energy absorption by CFRP composites are shown in Fig. 12. Inspection of Fig. 12 reveals that the increase in ductility is directly related to the increase in the number of layers of CFRP sheets. Also, Fig. 12 shows that the increase in ductility is directly related to decrease of compressive strength due to thermal shock. This indicated that damaged columns exhibited greater ductility than un-damaged columns. Whereas the ductility behavior (Stabilization of the ductility) of damaged and un-damaged columns decrease after seven and four layers of CFRP sheets, respectively, which can be classified as maximum amount for adequate ductility.

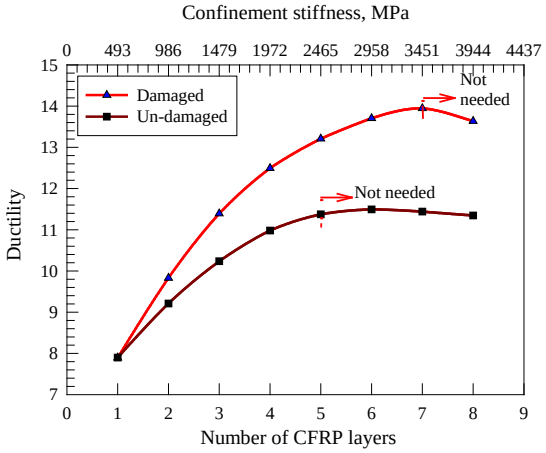

Figure 12. Increase in ductility versus number of CFRP layers.

3.6. Amount of CFRP for sufficient confinement and ductility

Fig. 13 shows the number of CFRP layers required for sufficient ductility and confinement versus concrete compressive strength. Based on the dilation properties and column ductility shown in Fig. 13, the maximum and minimum amount of CFRP were three and seven, respectively, of CFRP for damaged column and seven layers of CFRP for un-damaged columns, respectively. Also, Fig. 13 shows that number of CFRP layers controlled the behavior of the columns with concrete compressive strength less than 29 MPa, which indicated that there are maximum and minimum amount of CFRP to satisfy the ductility and confinement properties. On the other hand, for column with concrete compressive strength more than 29 MPa, the behavior was controlled by concrete compressive strength, which reflected that there is a fixed point for required number of CFRP layers for adequate ductility and confinement properties.

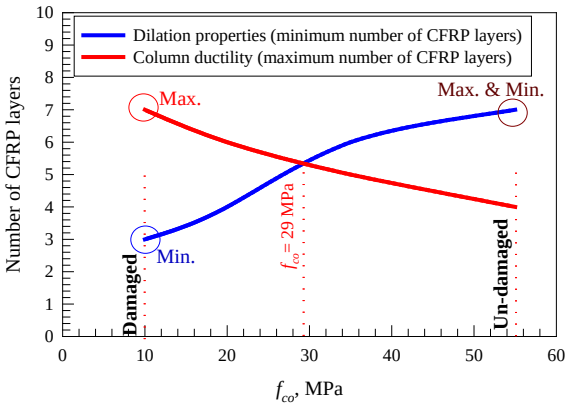

Figure 13. Number of CFRP layers versus unconfined strength of concrete.

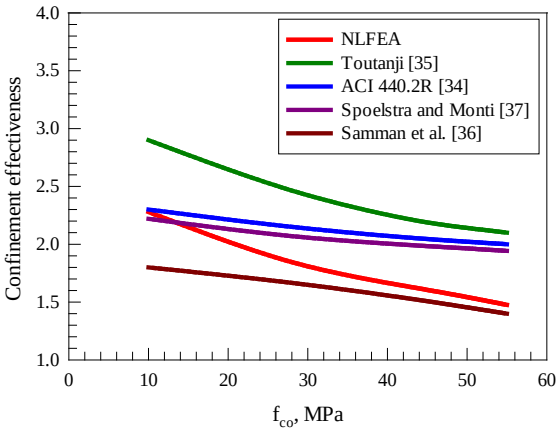

Figure 14. Effect of unconfined strength of concrete on confinement effectiveness.

3.7. Confinement effectiveness

Fig. 14 shows a plot of confinement effectiveness (ultimate load capacity of strengthened column divided by the ultimate load capacity of control column (un-strengthened)) versus the concrete compressive strength for confined column with one layer of CFRP composite. Also, Fig. 14 shows the predicted trends of the confinement effectiveness using ACI 440.2R [34], Toutanji [35], Samman et al. [36] and Spoelstra and Monti [37]. It is evident that as concrete compressive strength increases, confinement effectiveness decreases. The CFRP wrapped damaged columns show the maximum increases in ultimate load capacity. In addition, Fig. 14 shows that the confinement effectiveness of NLFEA columns is in good agreement with ACI 440.2R [34] and Samman et al. [36] damaged and un-damaged, respectively, but Toutanji [35] overestimated the predicted values by NLFEA columns. Fig. 15 shows the effect of concrete compressive strength on the confinement effectiveness or strength enhancement ratio. Inspection of Fig. 15 reveals that confinement effectiveness increased with the decrease of concrete compressive strength of damaged column. Also, Fig. 15 shows that, for relatively damaged, the increase of number of CFRP layers had a significant impact on the confinement effectiveness, which indicated that the ultimate behavior depends only on confinement effectiveness. This effect is insignificant in un-damaged columns, where only marginal increases in confinement effectiveness regardless of the number of layers, which indicated the confinement efficiency does not depend on the confinement level similar to conclusions observed by Issa and Tobaa [3].

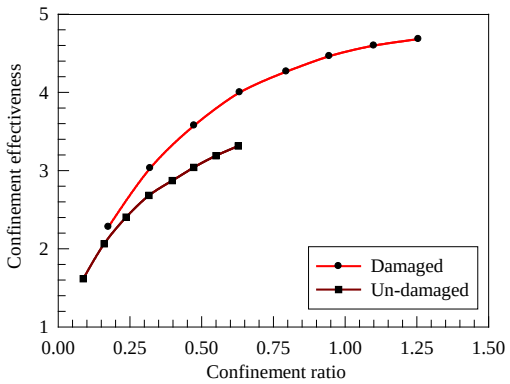

Figure 15. Confinement effectiveness versus confinement ratio.

4. Conclusions

1. The failure mode of the confined RC columns was sudden in the form of CFRP sheet fracture at the mid-height of the specimen followed by the fracturing of the lateral reinforcement and buckling of the longitudinal reinforcement. In the unconfined columns, the failure mode was also sudden due to the fracture of the lateral reinforcement and the outer concrete shell followed by buckling of the longitudinal reinforcement.

2. The axial load versus axial displacement curves of RC circular columns confined with CFRP composites are characterized by three stages. These three stages are the concrete has less expansion and fiber takes little constraining effect (Stage A), the concrete began to have a large expansion and the fiber begins to be stressed and crushing of the concrete at the end of this stage (Stage B), and the load was carried by the CFRP composite after crushing of the concrete until the fiber fractures (Stage C).

3. The influence of the number of CFRP layers on the ductility, energy absorption, and ultimate load improvement percentage is significant. There will be no further significant increase in the ductility and ultimate load of the column after a certain volumetric ratio, while significant increase in its stiffness continues to occur.

4. Thermal shock has a significant impact on the behavior of CFRP-confined circular RC columns. The increase in ductility is directly related to a decrease of compressive strength due to thermal shock. Also, the confinement effectiveness in terms of ultimate load was decreased with the increase in concrete compressive strength (un-damaged).

References

1. Mirmiran, A., Shahawy, M., Samaan, M., El-Echary, H. Effect of column parameters on FRP-confined concrete. J. Compos. Constr. 1998. 2 (4). Pp. 175–185. DOI: 10.1061/(ASCE)1090-0268(1998)2:4(175)
2. Parvin, A., Wang, W. Behavior of FRP jacketed concrete columns under eccentric loading. J. Compos. Constr. 2001. 5 (3). Pp. 146–152. DOI: 10.1061/(ASCE)1090-0268(2001)5:3(146)
3. Issa, M., Tobaa, H. Strength and ductility enhancement in high-strength confined concrete. Magazine of Concrete Research. 1994. 46 (168). Pp. 177-189. DOI: 10.1680/macr.1994.46.168.177
4. Kodur, V.K.R., Agrawal, A. An approach for evaluating residual capacity of reinforced concrete beams exposed to fire. Engineering Structures. 2016. 110 (1). Pp. 293–306. DOI: 10.1016/j.engstruct.2015.11.047
5. Al-Ostaz, A., Irshidat, M., Tenkhoff, B., Ponnapalli, P.S. Deterioration of bond integrity between repair material and concrete due to thermal and mechanical incompatibilities. Journal of Materials in Civil Engineering. 2010. 22 (2). Pp. 136–144. DOI: 10.1061/(ASCE)0899-1561(2010) 22:2(136)
6. Nedviga, E., Beresneva, N., Gravit, M., Blagodatskaya, A. Fire Resistance of Prefabricated Monolithic Reinforced Concrete Slabs of “Marko” Technology. Adv. Intell. Syst. Comput. 2018. 692 (1). Pp. 739–749. DOI: 10.1007/978-3-319-70987-1_78
7. Hezhev, T.A., Zhurtov, A.V., Tsipinov, A.S., Klyuev, S.V. Fire resistant fibre reinforced vermiculite concrete with volcanic application. Mag. Civ. Eng. 2018. 80 (1). Pp. 181–194. DOI:10.18720/MCE.80.16
8. Goremikins, V., Blesak, L., Novak, J., Wald, F. Experimental investigation on SFRC behaviour under elevated temperature. J. Struct. Fire Eng. 2017. 8 (1). Pp. 287–299. DOI: 10.1108/JSFE-05-2017-0034
9. Goremikins, V., Blesak, L., Novak, J., Wald, F. To testing of steel fibre reinforced concrete at elevated temperature. Appl. Struct. Fire Eng. 2017. DOI: 10.14311/asfe.2015.055
10. Blesak, L., Goremikins, V., Wald, F., Sajdlova, T. Constitutive model of steel fibre reinforced concrete subjected to high temperatures. Acta Polytech. 2016. 56 (1). Pp. 417–424. DOI: 10.14311/AP.2016.56.0417
11. Korsun, V., Vatin, N., Franchi, A., Korsun, A., Crespi, P., Mashtaler, S. The strength and strain of high-strength concrete elements with confinement and steel fiber reinforcement including the conditions of the effect of elevated temperatures. Procedia Eng. 2015. 117 (1). Pp. 970–979. DOI: 10.1016/j.proeng.2015.08.192
12. Goremikins, V., Blesak, L., Novak, J., Wald, F. Experimental method on investigation of fibre reinforced concrete at elevated temperatures. Acta Polytech. 2016. 56 (1). Pp. 258–264. DOI: 10.14311/AP.2016.56.0258
13. Selyaev, V.P., Nizina, T.A., Balykov, A.S., Nizin, D.R., Balbalin, A.V. Fractal analysis of deformation curves of fiber-reinforced fine-grained concretes under compression. PNRPU Mech. Bull. 2016. 1 (1). Pp. 129-146. DOI: 10.15593/perm.mech/2016.1.09
14. Bily, P., Fladr, J., Kohoutkova, A. Finite Element Modelling of a Prestressed Concrete Containment with a Steel Liner. Proceedings of the Fifteenth International Conference on Civil, Structural and Environmental Engineering Computing. Civil-Comp Press. 2015. DOI: 10.4203/ccp.108.1
15. Bílý, P., Kohoutková, A. Sensitivity analysis of numerical model of prestressed concrete containment. Nucl. Eng. Des. 2015. 295 (1). Pp. 204–214. DOI: 10.1016/j.nucengdes.2015.09.027
16. Al-Rousan, R. Behavior of two-way slabs subjected to drop-weight. Magazine of Civil Engineering. 2019. 90 (6). Pp. 62–71. DOI: 10.18720/MCE.90.6
17. Al-Rousan, R. The impact of cable spacing on the behavior of cable-stayed bridges. Magazine of Civil Engineering. 2019. 91 (7). Pp. 49–59. DOI: 10.18720/MCE.91.5
18. Krishan, A., Rimshin, V., Erofeev, V., Kurbatov, V., Markov, S. The energy integrity resistance to the destruction of the long-term strength concrete. Procedia Eng. 2015. 117 (1). Pp. 211–217. DOI: 10.1016/j.proeng.2015.08.143
19. Bily, P., Kohoutková, A. Numerical analysis of anchorage between steel liner and prestressed nuclear containment wall. Proc. 10th fib Int. PhD Symp. Civ. Eng. 2014. 529–534.
20. Korsun, V., Vatin, N., Korsun, A., Nemova, D. Physical-mechanical properties of the modified fine-grained concrete subjected to thermal effects up to 200°S. Appl. Mech. Mater. 2014. 633–634. Pp. 1013–1017. DOI: 10.4028/www.scientific.net/AMM.633-634.1013
21. Korsun, V., Korsun, A., Volkov, A. Characteristics of mechanical and rheological properties of concrete under heating conditions up to 200°C. MATEC Web Conf. 2013. 6 (1). Pp. 07002. DOI: 10.1051/matecconf/20130607002

22. Petkova, D., Donchev, T., Wen, J. Experimental study of the performance of CFRP strengthened small scale beams after heating to high temperatures. Construction and Building Materials. 2014. 68 (1). Pp. 55–61. DOI: 10.1016/j.conbuildmat.2014.06.014
23. Ji, G., Li, G., Alaywan, W. A new fire resistant FRP for externally bonded concrete repair. Construction and Building Materials. 2013. 42 (1). Pp. 87–96. DOI: 10.1016/j.conbuildmat.2013.01.008
24. Trentin, C., Casas, J.R. Safety factors for CFRP strengthening in bending of reinforced concrete bridges. Composite Structures. 2015. 128 (1). Pp. 188–198. DOI: 10.1016/j.compstruct.2015.03.048
25. Ferrari, V.J., de Hanai, J.B., de Souza, R.A. Flexural strengthening of reinforcement concrete beams using high performance fiber reinforcement cement-based composite (HPFRCC) and carbon fiber reinforced polymers (CFRP). Construction and Building Materials. 2013. 48 (1). Pp. 485–498. DOI: 10.1016/j.conbuildmat.2013.07.026
26. Attari, N., Amziane, S., Chemrouk, M. Flexural strengthening of concrete beams using CFRP, GFRP and hybrid FRP sheets. Construction and Building Materials. 2012. 37 (1). Pp. 746– 757. DOI: 10.1016/j.conbuildmat.2012.07.052
27. Kara, I.F., Ashour, A.F., Körog˘lu, M.A. Flexural behavior of hybrid FRP/steel reinforced concrete beams. Composite Structures. 2015. 129(1). Pp. 111–121. DOI: 10.1016/j.compstruct.2015.03.073.
28. Kolchunov, V.I., Dem'yanov, A.I. The modeling method of discrete cracks in reinforced concrete under the torsion with bending. Magazine of Civil Engineering. 2018. 81 (5). Pp. 160–173. DOI: 10.18720/MCE.81.16
29. Travush, V.I., Konin, D.V., Krylov, A.S. Strength of reinforced concrete beams of high-performance concrete and fiber reinforced concrete. Magazine of Civil Engineering. 2018. No. 77 (1). Pp. 90–100. DOI: 10.18720/MCE.77.8
30. Issa, M.A., Alrousan, R., Issa, M. Experimental and Parametric Study of Columns with CFRP Composites. Journal of Composites for Construction ASCE. 2009. 13 (2). Pp. 135−147. DOI: 10.1061/(ASCE)1090-0268(2009)13:2(135)
31. Swesi, A.O. Repair of Shear-Deficient Normal Weight Concrete Beams Damaged by Thermal Shock Using Advanced Composite Materials. Master Thesis. 2011.
32. Zhang, Y.X., Bradford, M.A. Nonlinear analysis of moderately thick reinforced concrete slabs at elevated temperatures using a rectangular layered plate element with Timoshenko beam functions. Engineering Structures. 2007. 29(10). Pp. 2751-2761. DOI: 10.1016/j.engstruct.2007.01.016
33. Haddad, R.H., Al-Rousan, R.Z. An anchorage system for CFRP strips bonded to thermally shocked concrete. International Journal of Adhesion and Adhesives. 2016. 71(1). Pp. 10−22. DOI: 10.1016/j.ijadhadh.2016.08.003
34. ACI Committee 440. Design and Construction of Externally Bonded FRP Systems for strengthening Concrete Structures. *ACI440.2R-02. 2002. American Concrete Institute, Farmington Hills, Mich.: 45 p. DOI: 10.1061/40753(171)159
35. Toutanji, H. Stress-strain characteristics of concrete columns externally confined with advanced fiber composite sheets. ACI Materials Journal. 1999. 96 (3). Pp. 397-404. DOI: 10.14359/639
36. Samaan, M., Mirmiran, A., Shahawy, M. Model of concrete confined by fiber composites. Journal of Structural Engineering. 1998. 124(9). Pp. 1025−1031. DOI: 10.1061/(ASCE)0733-9445(1998)124:9(1025)
37. Spoelstra, M., Monti, G. FRP-confined concrete model. Journal of Composites for Construction. 1999. 3(3). Pp. 143−150. DOI: 10.1061/(ASCE)1090-0268(1999)3:3(143)

Contacts:

Rajai Al-Rousan, rzalrousan@just.edu.jo